

Original Article



Combined Effects of 50 Hz Magnetic Field and Magnetic Nanoparticles on the Proliferation and Apoptosis of PC12 Cells*

JIA Hong Li^{1,2}, WANG Chao^{1,3}, LI Yue¹, LU Yan¹, WANG Ping Ping¹, PAN Wei Dong¹, and SONG Tao^{1,#}

1. Beijing Key Laboratory of Bioelectromagnetism, Institute of Electrical Engineering, Chinese Academy of Sciences, Beijing 100190, China; 2. University of Chinese Academy of Sciences, Beijing 100190, China; 3. Department of Basic Theory, Shandong Sport University, Jinan 250102, Shandong, China

Abstract

Objective To investigate the bioeffects of extremely low frequency (ELF) magnetic field (MF) (50 Hz, 400 μ T) and magnetic nanoparticles (MNPs) via cytotoxicity and apoptosis assays on PC12 cells.

Methods MNPs modified by SiO₂ (MNP-SiO₂) were characterized by transmission electron microscopy (TEM), dynamic light scattering and hysteresis loop measurement. PC12 cells were administrated with MNP-SiO₂ with or without MF exposure for 48 h. Cytotoxicity and apoptosis were evaluated with MTT assay and annexin V-FITC/PI staining, respectively. The morphology and uptake of MNP-SiO₂ were determined by TEM. MF simulation was performed by Ansoft Maxwell based on the finite element method.

Results MNP-SiO₂ were identified as ~20 nm (diameter) ferromagnetic particles. MNP-SiO₂ reduced cell viability in a dose-dependent manner. MF also reduced cell viability with increasing concentrations of MNP-SiO₂. MNP-SiO₂ alone did not cause apoptosis in PC12 cells; instead, the proportion of apoptotic cells increased significantly under MF exposure and increasing doses of MNP-SiO₂. MNP-SiO₂ could be ingested and then cause a slight change in cell morphology.

Conclusion Combined exposure of MF and MNP-SiO₂ resulted in remarkable cytotoxicity and increased apoptosis in PC12 cells. The results suggested that MF exposure could strengthen the MF of MNPs, which may enhance the bioeffects of ELF MF.

Key words: Extremely low frequency magnetic field; Magnetic nanoparticles; Cytotoxicity; Apoptosis; Morphology

Biomed Environ Sci, 2014; 27(2): 97-105

doi: 10.3967/bes2014.022

ISSN: 0895-3988

www.besjournal.com (full text)

CN: 11-2816/Q

Copyright ©2014 by China CDC

INTRODUCTION

Magnetic nanoparticles (MNPs) have been found in many organisms, such as magnetotactic bacteria^[1], pigeons^[2], honeybees^[3], and trout^[4]. It was reported that MNPs may be associated with the navigation and orientation of organisms^[5]. Interestingly, MNPs

have been detected in the human brain^[6], especially in the hippocampus^[7]. Additionally, there are many kinds of natural and artificial MNPs that can enter human body. Some epidemiological studies showed that there might be a link between extremely low frequency (ELF) magnetic field (MF) exposure and some central nervous system (CNS) diseases such as Alzheimer's disease (AD) and childhood leukemia.

*This work was supported by the State Key Development Program for Basic Research of China (2011CB503702) and the Key Program of National Natural Science of China (51037006).

#Correspondence should be addressed to: SONG Tao, PhD, professor; Tel/Fax: 86-10-82547164; E-mail: songtao@mail.iese.ac.cn
Biographical note of the first author: JIA Hong Li, female, born in 1976, Doctor candidate, majoring in Bioelectromagnetics.

Received: July 5, 2013;

Accepted: October 18, 2013

Thus, MNPs has been proposed to mediate the bioeffects of weak ELF MF on human tissues^[8-12]. According to general models, magnetite was found to oscillate and change the magnetic torque/force with ELF MF and cause a transient opening of the ion channel. However, such bioeffects induced by weak ELF MF exposure were determined theoretically, and there are still many disputes on the exact mechanisms^[13-14]. Furthermore, the exact threshold of when magnetic field exposure becomes a health hazard remains uncertain.

It is believed that the high magnetic permeability of MNPs can strengthen the MF around its surface. Binhi^[15] calculated the MF strengths around different sizes of MNP and analyzed the relationship between the magnitude of the MF and the free radical concentration according to the radical-pair reaction mechanism. Based on the amplification effects of the magnetic particles, he considered that the superparamagnetic nanoparticles might mediate the increasing risk of leukemia caused by environmental exposure to weak ELF MF. However, there were no experimental results to confirm his idea. To apply FeOx nanoparticles to liver cancer therapy, Ju et al.^[16] also reported that the combination of alternating MF (100 Hz, 670 μ T) and nanoparticles affected cell proliferation, apoptosis, and DNA metabolism while the nanoparticles alone did not induce significant effects. In addition, it was reported that static MF could exacerbate the cellular toxicity of MNPs^[17]. However, the combined biological effects and mechanisms of MNPs and power-frequency (50/60 Hz) MF in the environment are still not well studied.

We used the highly differentiated rat pheochromocytoma cell line PC12 in this study. The PC12 cells express NGF receptors, display neural characteristics and are the usual cell model in neurobiology studies. In view of the theoretical foundation described above, artificial MNPs were used to determine whether there were combined or amplified biological effects on the PC12 cells under alternating MF (50 Hz, 400 μ T).

MATERIALS AND METHODS

Cell Lines, Reagents, and Culture Conditions

The differentiated rat pheochromocytoma cell line PC12 (catalog number: TCR9) was purchased from the Cell Resource Center of Shanghai Institute of Biological Sciences, Chinese Academy of Sciences

(Shanghai, China). Dulbecco's modified Eagle medium (DMEM, high-glucose) and horse serum were purchased from Gibco (Grand Island, NY, USA). 3-(4,5)-dimethylthiazoliumromide (MTT) and penicillin/streptomycin were provided by Amresco (Solon, OH, USA). Dimethyl sulfoxide (DMSO) was obtained from Sigma-Aldrich (Munich, Germany). Fetal bovine serum (FBS) was supplied by Hangzhou Sijiqing Biological Engineering Materials Company (Hangzhou, China). The Annexin V-fluorescein isothiocyanate (FITC)/Propidium iodide (PI) kit was purchased from KeyGEN Biotech (Nanjing, China). MNPs modified by SiO₂ (MNP-SiO₂) in ethanol were provided by Wuhan WaWaSye Nanotech Company (Wuhan, China). Other reagents were of analytical grade and obtained from Beijing Chemical Works (Beijing, China).

The PC12 cells were routinely cultured with DMEM that was supplemented with 10% FBS, 5% horse serum, 100 IU/mL penicillin, and 100 μ g/mL streptomycin (hereafter called 'complete cell culture medium') in 95% air and 5% CO₂ at 37 °C. Cell passages were performed every three days. For MNP and ELF MF exposure, PC12 cells were seeded in 24-well plates at a density of 5 \times 10⁴ cells/well. The plates were then placed in a 5% CO₂ incubator at 37 °C for 24 h. The complete cell culture medium was replaced with a fresh one containing MNP-SiO₂ at final concentrations of 0, 20, and 100 μ g/mL, respectively. The cells treated with MNP-SiO₂ were cultured with or without MF exposure for another 48 h prior to the follow-up experiments.

Magnetic Field Exposure System

An alternating MF exposure system was developed in our laboratory^[18] using a double-wrapped coil system^[8,18] that consisted of an alternating power source and two solenoid coils (Figure 1). Each solenoid coil was composed of a core cylindrical tube of epoxy resins (inner diameter 200 mm, length 350 mm) and two subcoils with 160 turns each of enamel copper wire (diameter 2.06 mm) that could produce a MF with the same magnetic strength. If the alternating power source generated currents through the two subcoils in the same direction, an alternating MF would be produced. In the experiments, the applied current was 50 Hz, 0.4 A (root mean square value, or rms), and the corresponding magnetic field was 50 Hz, 400 μ T (rms). However, if the currents in the subcoils travelled in opposite directions, the alternating magnetic field intensity would be approximately 0 μ T

(less than 200 nT). The MF apparatus could be controlled by a switch with one coil generating an MF (experimental coil) and the other coil generating no MF (sham coil). The experimental and sham coils produced the same amount of heat, which would exclude any thermoeffects during exposure.

The two solenoid coils were placed into two CO₂ incubators prior to the experiments. The magnetic flux density and frequency in the solenoid were measured by an electromagnetic field analyzer (EFA-300, Wandel & Goltermann, Eningen, Germany). The direction of the MF of the experimental coil was vertical. Two nonmagnetic electronic thermometers (thermocouples) were placed in the two solenoid coils separately and used to monitor the temperature in the incubators in real time. Temperature was set at 37±0.1 °C. The intensities of the geomagnetic field in the vertical, north-south, and west-east directions were determined as 32, 21, and 9 μT, respectively, using a fluxgate magnetometer (CTM-5W01B, National Institute of Metrology, Beijing, China).

The experimental and sham groups were randomly selected by the designer at the start of the experiment. The operator was not informed of the selection to ensure the reliability of the results.

Preparation and Characterization of MNP-SiO₂

After drying and weighing, the MNP-SiO₂ particles were sterilized under ultraviolet radiation for at least 30 min. The particles were then suspended in complete cell culture medium to prepare a 10 mg/mL stock solution. Dispersion of particles was facilitated using 10 min of sonication in a water bath with an output power of 300 W at room temperature. Work solutions were prepared by

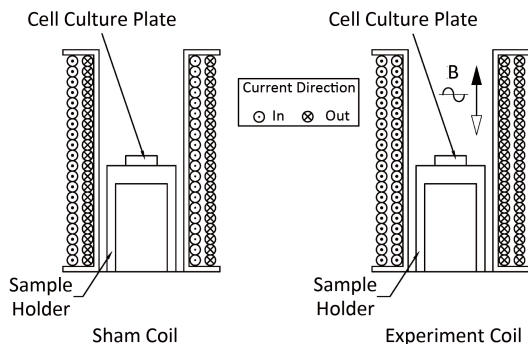


Figure 1. Schematic diagram of magnetic field orientation and position of sample holder during exposure.

diluting the stock solution immediately before the cellular administration of MNP-SiO₂.

The morphology of MNP-SiO₂ was determined under a Hitachi H-7650B transmission electron microscope (TEM) (Hitachi, Tokyo, Japan). MNP-SiO₂ were dried by N₂, resuspended with ddH₂O and sonicated as above. The MNP-SiO₂ solution was then mounted on a carbon grid. The morphological observation via TEM was performed at an acceleration voltage of 80 kV. The images were taken in ×40 K using a charge-coupled device camera with an AMT (Advanced Microscopy Techniques) Image Capture Engine Software (Danvers, MA, USA). The size of the MNP-SiO₂ was then determined.

The average hydrodynamic sizes of 100 μg/mL MNP-SiO₂ in distilled water and complete cell culture medium were measured using dynamic light scattering (DLS) (DynaPro NanoStar, Wyatt Technology Corporation, Santa Barbara, CA, USA) after sonicating for 10 min at 300 W. Each sample was measured three times with 10 acquisitions per measurement.

The magnetic hysteresis loop of MNP-SiO₂ after N₂ drying was measured at room temperature using an alternating gradient magnetometer (AGM model 2900, Princeton Measurements, Princeton, NJ, USA).

MNP-SiO₂ Uptake and TEM Morphology of PC12

The PC12 cells in a six-well plate were administrated with 0 μg/mL or 100 μg/mL MNP-SiO₂ (21.05 μg/cm², corresponding to 9.5 cm² surface area of the well) for 48 h, and any MNP-SiO₂ not attached to the cells were washed out with 0.1 mol/L phosphate buffer saline (PBS, pH 7.4). The cells were collected and fixed with 2.5% glutaraldehyde in 0.1 mol/L PBS (pH 7.4) for 30 min at room temperature and postfixed in 1% osmium tetroxide (pH 7.4). Then the cells were dehydrated in increasing grades of ethanol and embedded. Ultrathin sample sectioning was performed using a diamond knife, and the sections were observed under TEM.

MTT Assay

A modified MTT assay was used to assess the cytotoxicity of MNP-SiO₂ and ELF MF exposure on the PC12 cells. In brief, the PC12 cells were cultured on 24-well cell culture plastic plates overnight and were treated with different concentrations of MNP-SiO₂ with or without MF exposure (50 Hz, 400 μT) for 48 h. The same volumes of complete cell culture medium without the MNPs were added to

the control cells. Subsequently, 100 μL MTT stock solution (5 mg/mL in PBS, pH 7.4) was added into each well. After 1 h incubation at 37 °C, the medium in each well was removed carefully and replaced with 750 μL DMSO. The cell plates were shaken for 10 min to dissolve the formazan crystals completely. After centrifugation at 1 238 \times g for 5 min, 100 μL of supernatant was transferred from each well into a new 96-well plate. The absorbance of each sample in the 96-well plate was recorded at 570 nm using an iMark microplate absorbance reader (model 168-1 130, Bio-Rad Laboratories, Hercules, CA, USA). The relative cell viabilities of the MNP-SiO₂-treated cells were calculated as follows: relative viability (%) = (mean absorbance of MNP-SiO₂-treated cells / mean absorbance of untreated cells) \times 100.

Apoptosis Assay

The apoptosis assay was achieved by fluorescence-activated cell sorting (FACS) technique on a flow cytometer according to the Annexin V-FITC and PI Double Staining Apoptosis Detection Kit. In brief, the PC12 cells treated with MNP-SiO₂ were collected by trypsinization and washed twice with PBS. After resuspending the cells with the binding buffer (10 mmol/L HEPES, pH7.4, 140 mmol/L NaCl, 2.5 mmol/L CaCl₂), Annexin V-FITC and PI were added onto the cells successively. The cells were then incubated in the dark for 15 min at room temperature. FACS assay was used to detect cell apoptosis using the CyAn ADP (Advanced Digital Processing) 9 color flow cytometer (Beckman Coulter, Brea, CA, USA). The excitation wave length was 488 nm and the emission wave length was 530 nm. Untreated and H₂O₂-treated cells were used as the negative and positive controls, respectively, to eliminate any spectral overlap and delineate the quadrants for the different cell populations. A total of 20 000 to 30 000 cells were analyzed per sample, and the assay was performed four times. The living cells were Annexin V-FITC and PI double-negative, whereas the late apoptotic or secondary necrotic cells were double-positive. The early apoptotic cells were only Annexin V-FITC positive, whereas the isolated nuclei or cellular debris were only PI positive^[19].

Statistical Analysis

All statistical analyses were performed using SPSS version 11.5 (SPSS, IBM, Chicago, IL, USA). All data were presented as mean \pm standard error of the mean (SEM), except for the DLS, where data were

presented as mean \pm standard deviation (SD).

To analyze the MTT assay results, a paired *t*-test was used to compare the mean absorbance (A) values of six replicates of nine MF and sham experiments with the same concentrations of MNP-SiO₂. The equation $\lg[A/A_{(\text{sham},0)}]$ was used to establish the homogeneity of variance, where $A_{(\text{sham},0)}$ was the absorbance of the sham group with 0 $\mu\text{g}/\text{mL}$ MNPs-SiO₂. Two-way ANOVA was then used to analyze the effects of MF and MNP-SiO₂ concentration. One-way ANOVA was used to investigate the difference between the rate of cell growth with an index, $(A_{\text{MF}} - A_{\text{sham}})/A_{\text{sham}}$, followed with a post-hoc test (Bonferroni) to denote the role of MF at the same concentration of MNP-SiO₂.

For the FACS assays, a statistical analysis of the percentage of apoptotic cells was performed via two-way ANOVA to determine the effects of MF exposure and MNP-SiO₂. One-way ANOVA and post-hoc test (Bonferroni) were performed to compare the different apoptosis rates of three MNP-SiO₂ concentrations in the MF or sham group. Student's *t*-test was used to compare the apoptotic rates in the MF and sham groups at the same MNP-SiO₂ concentration.

$P < 0.05$ was considered statistically significant in all statistical tests.

RESULTS

Morphology of MNP-SiO₂

TEM analysis (Figure 2A) found that MNP-SiO₂ have a spherical shape and range (diameter) from 15 nm to 45 nm in size, with most at 15 nm to 20 nm. A uniform layer (4.35 nm average thickness) of SiO₂-modified groups surrounded the MNPs.

The hydrodynamic diameters of MNP-SiO₂ dispersed in distilled water and complete cell culture medium were 432.28 ± 25.17 nm ($n=30$) and 530.37 ± 63.51 nm ($n=30$) by DLS measurement, respectively. These results suggested that the particle suspensions in water or complete culture medium were mainly composed of aggregates^[20].

The magnetic hysteresis loop of MNP-SiO₂ was measured at room temperature (Figure 2B). The coercive force was 11.75 kA/m, indicating that the magnetic particles were ferromagnetic materials, which were similar to the endogenous magnetic particles found in the upper beak skin of adult homing pigeons^[11,21].

Calculation of MF around the MNPs

The MF with MNP-SiO₂ (20 nm diameter) was calculated using the finite element method and Ansoft Maxwell software (Version 13.0.0, ANSYS, Canonsburg, USA), as shown in Figure 3. The calculated distribution of MF was at the moment when alternating MF changed to 400 μT. The results showed that the region with a higher MF intensity increased with increasing magnetic particles, suggesting that more cells were exposed at higher MF. Nanoparticles are prone to aggregate, as explained in Figure 2A and the hydrodynamic diameter; therefore, the range and intensity of the MF surrounding the nanoparticle aggregates will be higher than found in the calculation. The bioeffects of high-intensity MF are more significant^[32-34]; thus, in theory, the biological effects of MF on cells can be enhanced with increasing MNP-SiO₂ concentration (i.e. the combined effects are more significant since MNPs amplify the intensity of the external MF even though MNP or MF alone has no effects on the cells).

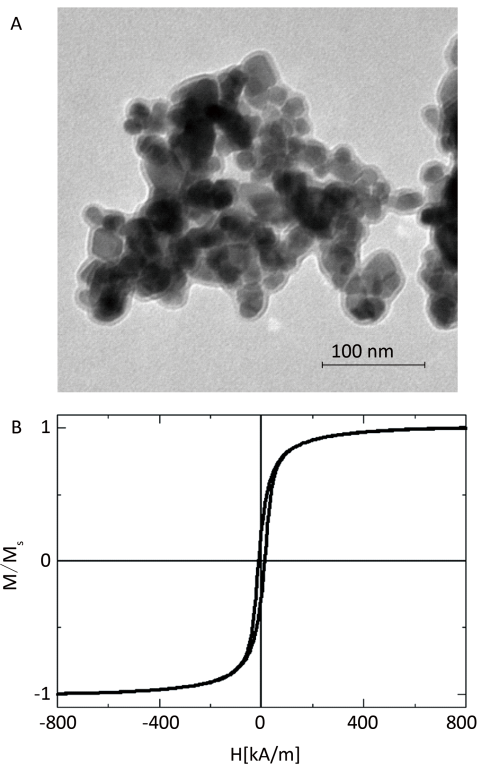


Figure 2. MNP-SiO₂ characterization. (A) Transmission electron microscope image of MNP-SiO₂. (B) Magnetic hysteresis loop of MNP-SiO₂.

Cytotoxicity of MF and MNP-SiO₂

Forty-eight hours of MNP-SiO₂ yielded dose-dependent cytotoxicity (Figure 4), as determined by MTT assay. The IC₅₀, the dose at which 50% of cells remain viable relative to the untreated cells, of MNP-SiO₂ was over 8 000 μg/mL, indicating that MNP-SiO₂ exhibited weak toxicity on PC12 cells. Subsequent experiments assessed the combined cytotoxicity of MF and 0 μg/mL, 20 μg/mL (5.26 μg/cm²), and 100 μg/mL (26.32 μg/cm²) MNP-SiO₂ which resulted in 100%, >90%, and >80% cell viability, respectively.

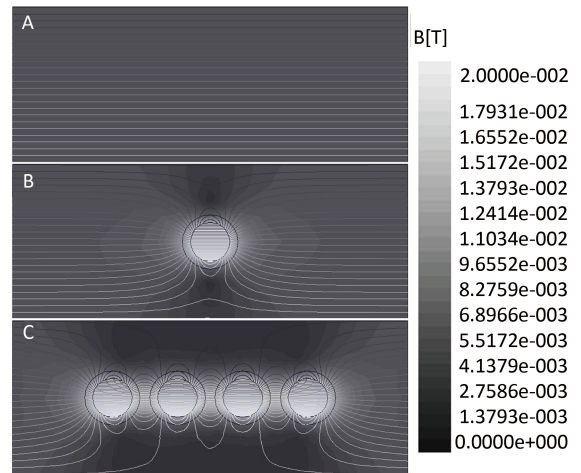


Figure 3. Distribution of the MF of 20 nm diameter magnetic particles under an external 400 μT MF: (A) no magnetic particles; (B) one particle; and (C) four particles.

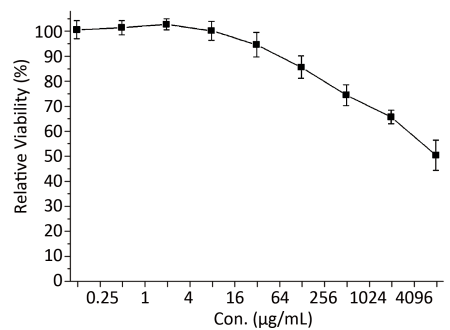


Figure 4. Dose-dependent curve of MNP-SiO₂ versus cell viability. MNP-SiO₂ cytotoxicity was determined using MTT assay. PC12 cells were cultured in a 24-well plate and exposed to different concentrations of MNP-SiO₂ for 48 h. The results are expressed as percent cell viability (compared with that of 0 μg/mL). Data are presented as mean±SEM (n=6).

The cytotoxicity assay was repeated nine times, with six replicates per group in each experiment. The mean absorbance values of the six replicates per group were used for a paired *t*-test ($n=9$). The results showed significantly reduced cell viability in the MF group with 100 $\mu\text{g}/\text{mL}$ MNP-SiO₂ compared with that in the sham group ($P<0.05$). No significant differences between the MF and sham groups were observed in the 0 $\mu\text{g}/\text{mL}$ ($P>0.05$) and 20 $\mu\text{g}/\text{mL}$ MNP-SiO₂ ($P>0.05$) groups (Figure 5A).

Two-way ANOVA was used to analyze the effects of MF exposure and MNP-SiO₂. The equation $\lg[A/A_{(\text{sham},0)}]$ was used for the homogeneity of variance, where $A_{(\text{sham},0)}$ was the absorbance of the

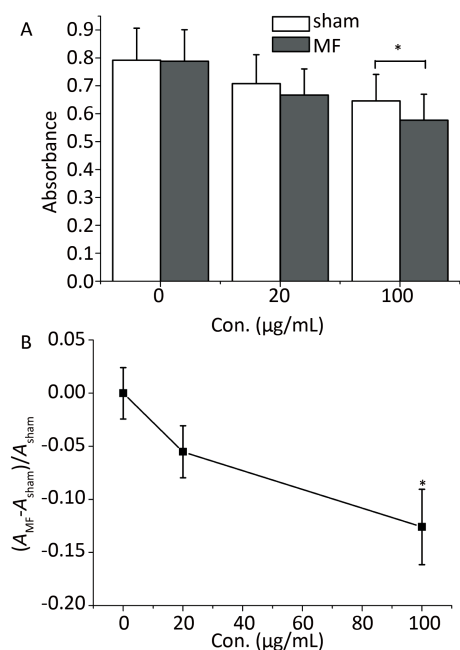


Figure 5. Cytotoxicity of MF and MNP-SiO₂ on PC12 cells determined using MTT assay. Data are presented as mean \pm SEM. PC12 cells were treated MNP-SiO₂ with or without MF exposure in a 24-well plate for 48 h. The absorbance values were read at 570 nm. Nine independent experiments and six replicates per MNP-SiO₂ concentration were done. (A) MTT results for MF and MNP-SiO₂ on the PC12 cells. The mean absorbance values of the six replicates of the MF groups were compared with that of the sham groups at the same MNP-SiO₂ concentration using a paired *t*-test ($n=9$), * $P<0.05$. (B) The rate of cell growth compared with that of the sham group. The equation $(A_{\text{MF}} - A_{\text{sham}}) / A_{\text{sham}}$ was used for one-way ANOVA ($n=9$) analysis, * $P<0.05$ (compared with the 0 $\mu\text{g}/\text{mL}$ group).

sham group with 0 $\mu\text{g}/\text{mL}$ MNPs-SiO₂. The results showed that MF ($P<0.01$) and MNP-SiO₂ ($P<0.01$) both exhibited significant effects on the viability of the PC12 cells. In addition, a significant interaction between MF and MNP-SiO₂ was observed ($P<0.05$).

To further determine the role of MF on PC12 cell viability, the equation $(A_{\text{MF}} - A_{\text{sham}}) / A_{\text{sham}}$ was used to determine how the viability of the MF group went relative to that of the sham group. A_{MF} was the absorbance value of the MF group, and A_{sham} was the absorbance value of the sham group. As shown in Figure 5B, MF exposure decreased cell growth as MNP-SiO₂ increased. One-way ANOVA showed a significant difference ($P<0.05$) between the 0, 20, and 100 $\mu\text{g}/\text{mL}$ MNP-SiO₂ groups. A post hoc test found a significant difference ($P<0.05$) between the 100 and 0 $\mu\text{g}/\text{mL}$ groups while there was no difference between the 20 and 0 $\mu\text{g}/\text{mL}$ groups.

MNP-SiO₂ Uptake via TEM

TEM analysis was used to determine whether MNP-SiO₂ particles were taken up by PC12 cells. Figure 6 shows that some MNPs adhered to the cell surfaces (Figure 6D), while others were ingested into the cells and dispersed into cytoplasm as clusters (Figure 6B, 6C) or individual particles (Figure 6D) with or without membrane binding. The MNP-SiO₂ entered the cells by endocytosis or direct penetration (Figure 6D). Most of the particles were aggregated, as shown in the electron dense regions in the cytoplasm (Figure 6B, 6C). The mitochondrion and the cell nucleus remained intact, and the chromatin dispersed nonhomogeneously compared with that of the untreated cell (Figure 6A).

Detection of Apoptosis of the PC12 Cells

To identify whether MF exposure and MNP-SiO₂ induced apoptosis, the treated cells were stained with Annexin V-FITC/PI. An increase in the FITC-conjugated Annexin V-positive cells is an early marker for apoptosis^[19]. PI staining was used to investigate the loss of cell membrane integrity (Figure 7A).

The rate of apoptosis in PC12 cells (i.e., the proportion of Annexin V⁺ cells) was shown in Figure 7B. Two-way ANOVA revealed that MF ($P<0.01$) exposure had a significant effect on the apoptosis of PC12 cells while MNP-SiO₂ did not ($P>0.05$). Neither was there significant interaction between MF exposure and MNP-SiO₂ ($P>0.05$). The Student's *t*-test was performed to compare the rate of apoptosis in the MF and sham groups at the same

MNP-SiO₂ concentration. Significant differences were observed between the MF and sham groups treated with 100 ($P<0.01$) and 20 $\mu\text{g/mL}$ MNP-SiO₂ ($P<0.05$) (Figure 6B). One-way ANOVA was performed to compare the rates of apoptosis between the three MNP-SiO₂ concentrations in the MF or sham group. The results showed statistically significant differences ($P<0.05$) in the apoptotic rates

of the different MNP-SiO₂ concentrations in the MF groups, but not in the sham group ($P>0.05$). Bonferroni analysis revealed significant differences between 100 $\mu\text{g/mL}$ and 0 $\mu\text{g/mL}$ ($P<0.05$) in the MF group (Figure 7B). It was also found that the apoptotic rates in the MF group increased with MNP-SiO₂ concentration, while the sham group did not show a similar trend.

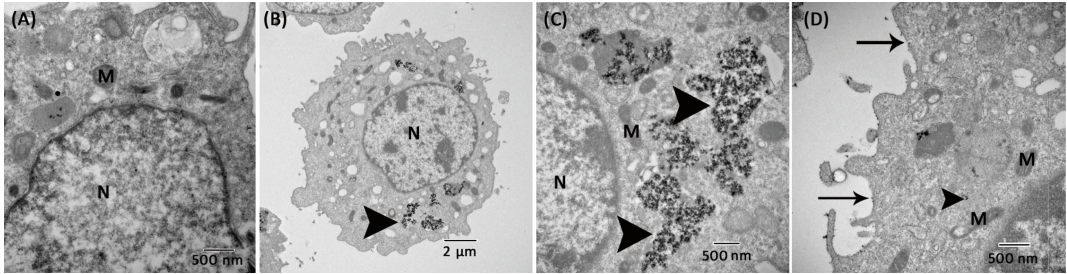


Figure 6. TEM morphology of the MNP-SiO₂-treated PC12 cells. (A) Untreated PC12 cells; (B), (C), and (D): PC12 cells treated with 100 $\mu\text{g/mL}$ MNP-SiO₂. N: nucleus; M: mitochondrion; arrows: MNP-SiO₂ engulfed into the cell or adhered to the cell membrane; hollow arrowhead: location of MNP-SiO₂ in the cells.

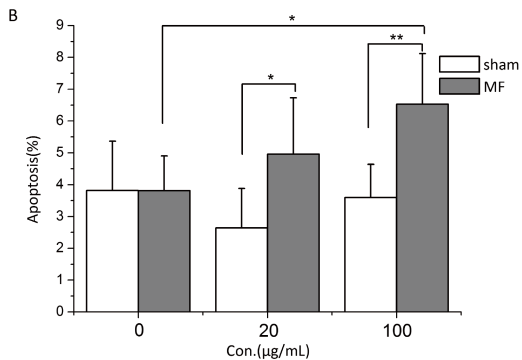
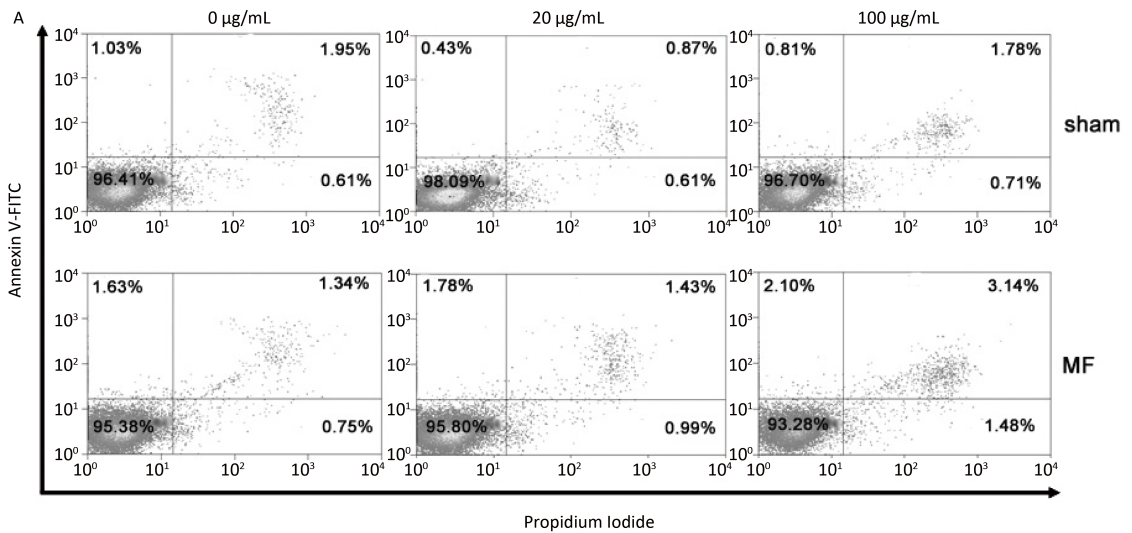


Figure 7. Detection of apoptosis in PC12 cells. (A) Flow cytometry results: lower left quadrants show the viable cells (Annexin V/Pi); upper right quadrants contain the late apoptotic and secondary necrotic cells (Annexin V*Pi); upper left quadrants contain the apoptotic cells (Annexin V*Pi). (B) Proportion of apoptotic PC12 cells evaluated using Annexin V⁺ cells in flow cytometry assay. Data are presented as mean \pm SEM ($n=16$) with * $P<0.05$ and ** $P<0.01$.

DISCUSSION

With the increasing use of electrical equipment, the biological effects of electromagnetic field have become a public concern. Epidemiological investigations displayed a correlation between ELF MF exposure and CNS diseases, such as AD^[22-23] and childhood leukemia^[24]. The concentration of MNPs in the brain of AD patients was found to be much higher than that in the control group^[25]. MNPs can appear in biological tissues through biomineralization, but natural and artificial MNPs can also penetrate through cell membranes and increase the risk of childhood leukemia^[15]. Thus, magnetic particles may be an ideal target for external ELF MF and play an important role in some CNS diseases. The present study used MNP-SiO₂ that was similar in size to the MNPs found in the human brain. The results showed that the particles adhered to the cell surfaces and entered the cells, evidencing that MNP-SiO₂ could simulate the endogenous biomagnetite to a certain extent.

Because MNPs have a wide range of applications in the biomedical field, there has been extensive research on the biosafety of MNPs. It was found that MNPs have different bioeffects on cell morphology, cytoskeleton, proliferation, functionality, viability, reactive oxygen species and cellular homeostasis^[26-27]. Our results showed that MNP-SiO₂ reduced cell viability dose-dependently, which was consistent with previous studies^[28]. Because flow cytometry analyses showed that MNP-SiO₂ alone did not induced significant apoptosis, the cytotoxicity of MNP-SiO₂ may have been caused by the cell membrane damaged from direct penetration of the nanoparticles. The combined bioeffects of MF and MNP-SiO₂ exposure were more obvious. The rate of cell growth decreased when exposed to MF and increasing doses of MNP-SiO₂, suggesting that the MF enhanced cytotoxicity when treated with higher concentrations of MNP-SiO₂. Apoptosis increased with increasing MNP-SiO₂ in the MF group while 0 µg/mL MNP-SiO₂ yielded no significant differences between the MF and sham groups. This indicated that the combined effect of MF and MNP-SiO₂ was more significant than MF or MNP-SiO₂ alone. It also should be noted that the MNP concentrations in our experiments might have exceeded the levels normally found in the human brain. Thus, the effects of MF on human health might be much weaker than what was observed in this study.

We noticed an inconsistent relationship

between the presence of apoptosis and cytotoxicity in the sham group. MTT is a substrate of the enzyme succinate dehydrogenase (SDH) in the mitochondria of live cells and is used to detect cell viability. It was reported that nanoparticles could impede the attachment of astrocytes to the substratum and cause mitochondrial stress^[29], which might affect the reaction of SDH and MTT. Furthermore, MNPs could arrest the cell cycle and inhibit proliferation as a type of stress factor. However, these effects would not cause cells to undergo active apoptosis. As MNPs would be expected to decrease cell viability but with no significant apoptosis, the contradictory results found in this study mean that further research is required to determine the exact mechanism involved.

Studies have shown that some kinds of strong magnetic fields enhance cellular and nuclear uptake as well as MNP aggregation^[17,30-31]. Aggregated MNPs themselves can cause cell death. Combined with increased uptake, their toxic effects may be even more significant^[17,31]. Few studies have investigated the impacts of ELF MF on nanoparticle uptake. Although we did not observe a significant increase in cellular uptake of nanoparticles under ELF MF exposure (data not shown), cytotoxicity and apoptosis from MF exposure increased significantly with increasing MNP-SiO₂. It should be noted that further studies are required to explore if ELF MF exposure increases MNP uptake and the mechanism that is involved in the combined apoptotic effects of ELF MF and MNPs.

The present experimental results suggest that the magnetic particles might induce and strengthen the ELF MF effects on cell proliferation and apoptosis as MNP-SiO₂ concentration increases. Binhi^[15] proposed that MNPs could generate their own MF which were orders of magnitude greater than the surrounding geomagnetic field (0.05 mT) generated by an external MF (the MF intensity was 1 mT to 200 mT within 100 nm around the magnetic particles). This implies that MNPs can enlarge the strength of the MF around their surface. Hence, it is reasonable to predict the amplified bioeffects of the applied magnetic field.

In conclusion, the presences of both ELF MF and MNPs demonstrate more significant combined biological effects than each one alone. This is consistent with the hypothesis that the nanoparticles exacerbate the biological effect of ELF MF by amplifying the MF strength. Therefore, MF can function through magnetic particles to exert its

bioeffects, implying that the magnetic particles themselves may play an important role in MF-related disorders. This finding may be helpful in understanding the process of diseases related to MF and MNPs.

ACKNOWLEDGEMENT

We thank all the technical staff in our laboratory for their work on the exposure system.

DECLARATION OF INTEREST

The authors report no conflicts of interest.

REFERENCES

- Blackmore R. Magnetotactic bacteria. *Science*, 1975; 190, 377-9.
- Walcott C, Gould JL, and Kirschvink JL. Pigeons have magnets. *Science*, 1979; 205, 1027-9.
- Hsu CY and Li CW. Magnetoreception in honeybees. *Science*, 1994; 265, 95-7.
- Walker MM, Diebel CE, Haugh CV, et al. Structure and function of the vertebrate magnetic sense. *Nature*, 1997; 390, 371-6.
- Johnsen S and Lohmann KJ. The physics and neurobiology of magnetoreception. *Nature Reviews Neuroscience*, 2005; 6, 703-12.
- Kirschvink JL, Kobayashi-kirschvink A, and Woodford BJ. Magnetite biomineralization in the human brain. *Proceedings of the National Academy of Sciences of the United States of America*, 1992; 89, 7683-7.
- Dunn JR, Fuller M, Zoeger J, et al. Magnetic material in the human hippocampus. *Brain Research Bulletin*, 1995; 36, 149-53.
- Kirschvink JL. Uniform magnetic-fields and double-wrapped coil systems-improved techniques for the design of bioelectromagnetic experiments. *Bioelectromagnetics*, 1992; 13, 401-11.
- Kirschvink JL, Walker MM, and Diebel C. Magnetite-based magnetoreception. *Current Opinion Neurobiology*, 2001; 11, 462-7.
- Davila AF, Fleissner G, Winklhofer M, et al. A new model for a magnetoreceptor in homing pigeons based on interacting clusters of superparamagnetic magnetite. *Physics and Chemistry of the Earth*, 2003; 28, 647-52.
- Fleissner G, Stahl B, Thalau P, et al. A novel concept of Fe-mineral-based magnetoreception: histological and physicochemical data from the upper beak of homing pigeons. *Naturwissenschaften*, 2007; 94, 631-42.
- Solov'yov IA and Greiner W. Theoretical analysis of an iron mineral-based magnetoreceptor model in birds. *Biophys J*, 2007; 93, 1493-509.
- Adair RK. Constraints of thermal noise on the effects of weak 60-Hz magnetic-fields acting on biological magnetite. *Proceedings of the National Academy of Sciences of the United States of America*, 1994; 91, 2925-9.
- Vanderstraeten J and Gillis P. Theoretical evaluation of magnetoreception of power-frequency fields. *Bioelectromagnetics*, 2010; 31, 371-9.
- Binh V. Do naturally occurring magnetic nanoparticles in the human body mediate increased risk of childhood leukaemia with EMF exposure? *International Journal of Radiation Biology*, 2008; 84, 569-79.
- Ju H, Dai Z, Sun M, et al. Effects on different diameter of nano-FeOx powders under external magnetic field on characteristics of heptoma-cell lines Bel-7402 *Journal of Jiangsu University (Medicine Edition)*, 2009; 19, 6.
- Bae JE, Huh MI, Ryu BK, et al. The effect of static magnetic fields on the aggregation and cytotoxicity of magnetic nanoparticles. *Biomaterials*, 2011; 32, 9401-14.
- Yang W, Huo X, and Song T. Effects of extremely low-frequency-pulsed electromagnetic field on different-derived osteoblast-like cells. *Electromagnetic Biology and Medicine*, 2008; 27, 298-311.
- van Engeland M, Nieland LJW, Ramaekers FCS, et al. Annexin V-affinity assay: A review on an apoptosis detection system based on phosphatidylserine exposure. *Cytometry*, 1998; 31, 1-9.
- Jiang J, Oberdorster G, and Biswas P. Characterization of size, surface charge, and agglomeration state of nanoparticle dispersions for toxicological studies. *Journal of Nanoparticle Research*, 2009; 11, 77-89.
- Treiber CD, Salzer MC, Riegler J, et al. Clusters of iron-rich cells in the upper beak of pigeons are macrophages not magnetosensitive neurons. *Nature*, 2012; 484, 367-U102.
- Feychting M, Pedersen NL, Svedberg P, et al. Dementia and occupational exposure to magnetic fields. *Scandinavian Journal of Work Environment & Health*, 1998; 24, 46-53.
- Sobel E, Davanipour Z, Sulkava R, et al. Occupations with exposure to electromagnetic fields: a possible risk factor for Alzheimer's disease. *American Journal of Epidemiology*, 1995; 142, 515-24.
- Ahlbom A, Day N, Feychting M, et al. A pooled analysis of magnetic fields and childhood leukaemia. *Br J Cancer*, 2000; 83, 692-8.
- Ott BR and Cahn-Weiner DA. Gender differences in Alzheimer's disease. *Geriatric Times*, 2001; 2, 23-4.
- Soenen SJH, Himmelreich U, Nuytten N, et al. Cytotoxic effects of iron oxide nanoparticles and implications for safety in cell labelling. *Biomaterials*, 2011; 32, 195-205.
- Naqvi S, Samim M, Abdin MZ, et al. Concentration-dependent toxicity of iron oxide nanoparticles mediated by increased oxidative stress. *International Journal of Nanomedicine*, 2010; 5, 983-9.
- Gaihre B, Khil MS, and Kim HY. *In vitro* anticancer activity of doxorubicin-loaded gelatin-coated magnetic iron oxide nanoparticles. *Journal of Microencapsulation*, 2011; 28, 286-93.
- Au C, Mutkus L, Dobson A, et al. Effects of nanoparticles on the adhesion and cell viability on astrocytes. *Biological Trace Element Research*, 2007; 120, 248-56.
- Lee CH, Chen CB, Chung TH, et al. Cellular Uptake of Protein-Bound Magnetic Nanoparticles in Pulsed Magnetic Field. *J Nanosci Nanotechnol*, 2010; 10, 7965-70.
- Smith CAM, de la Fuente J, Pelaz B, et al. The effect of static magnetic fields and tat peptides on cellular and nuclear uptake of magnetic nanoparticles. *Biomaterials*, 2010; 31, 4392-400.
- Saito A, Takayama Y, Moriguchi H, et al. Developmental effects of low frequency magnetic fields on P19-derived neuronal cells. *Engineering in Medicine and Biology Society*, 2009. EMBC 2009. Annual International Conference of the IEEE. 2009: 5942-5.
- Xu C, Fan Z, Chao YL, et al. Magnetic fields of 10 mT and 120mT change cell shape and structure of F-actins of periodontal ligament cells. *Bioelectrochemistry*, 2008; 72, 41-6.
- Yan J, Dong L, Zhang B, et al. Effects of extremely low-frequency magnetic field on growth and differentiation of human mesenchymal stem cells. *Electromagnetic Biology and Medicine*, 2010; 29, 165-76.